Synchronization of unidirectionally coupled multi-transverse-mode vertical-cavity surface-emitting lasers

Maria Susana Torre

Instituto de Física Arroyo Seco, Universidad Nacional del Centro de la Provincia de Buenos Aires Pinto 399, 7000 Tandil, Argentina

Cristina Masoller

Instituto de Física, Facultad de Ciencias, Universidad de la República, Igua 4225, Montevideo 11400, Uruguay, and School of Informatics, University of Wales, Bangor, Dean Street, Bangor LL57 1UT, UK

K. Alan Shore

School of Informatics, University of Wales, Bangor, Dean Street, Bangor LL57 1UT, UK

Received January 15, 2004; revised manuscript received May 12, 2004; accepted May 21, 2004

The synchronization of unidirectionally coupled multi-transverse-mode vertical-cavity surface-emitting lasers (VCSELs) is numerically studied. It is demonstrated that synchronization can be achieved between each transverse mode of a master laser and its counterpart, a slave laser. This result opens the opportunity for multichannel chaotic communications by use of multi-transverse-mode VCSELs. It is further shown that two distinct synchronization regimes exist, complete synchronization and injection locking, which can be distinguished by the lag time between the master and the slave laser intensities. © 2004 Optical Society of America

OCIS codes: 140.5960, 140.1540, 060.4510.

1. INTRODUCTION

The synchronization of chaotic lasers in a unidirectional coupling configuration (master–slave or transmitter–receiver) has received much attention in the last decade motivated by the potential application in secure optical communication systems.[1,2] Particular attention has been paid to the synchronization of edge-emitting semiconductor lasers that are key elements of optical communication systems. External optical feedback has been used to render the master laser chaotic.[3–17] For the slave laser, two different situations have been considered: either the slave laser is also subjected to optical feedback (a closed-loop configuration) or is a stand-alone, solitary laser (open-loop configuration). Recent research has focused on comparing advantages and drawbacks of these configurations for message encryption and decryption.[18,19]

In contrast with the significant achievements that have been made in the synchronization of edge-emitting semiconductor lasers, relatively little attention has been given to the synchronization of chaotic vertical-cavity surface-emitting lasers (VCSELs).[20,21] VCSELs are recognized as having many advantages over conventional, edge-emitting semiconductor lasers.[22] Because of their short cavity length VCSELs emit in a single-longitudinal mode. They have low threshold current, high efficiency, can be modulated at high speeds, are compact, can easily be formed in laser arrays, and have a narrow circular beam profile and thus can be efficiently coupled to an optical fiber. A drawback is their relatively low output power, which makes them difficult to synchronize. A recent experimental demonstration of synchronization of mutually coupled VCSELs was reported by Fujiwara *et al.*,[23] and of unidirectionally coupled VCSELs by Hong *et al.*[24] Such synchronization can be best achieved when the master VCSEL output power is large, i.e., when the master VCSEL is operated well above threshold. However, in marked contrast to edge-emitting lasers, for large bias currents a VCSEL generally operates in multiple transverse modes. It is thus of great importance to understand how multi-transverse-mode emission affects the synchronization of VCSELs. In this paper we show theoretically, by means of numerical simulations, that two multi-transverse-mode VCSELs in a master–slave configuration can be synchronized by an adequate amount of optical injection. We use a model that takes into account the spatial dependence of three transverse modes and of two carrier densities, associated with confined carriers in the quantum well region of the laser and unconfined carriers in the barrier region. Optical feedback in the master laser rate equations is included as in the Lang–Kobayashi model. The model is similar to that previously used by Yu *et al.*,[25] where two transverse modes were considered and the influence of the side mode on the performance of three different encoding methods (chaotic modulation, chaotic masking, and chaotic shift keying) by use of VCSELs was analyzed.

Here we focus on multimode behavior of VCSELs and show that both in-phase and antiphase properties of the

master laser modal intensities can be transferred to the slave laser. The results reported in this paper indicate that a functional advantage can be extracted from the rich dynamics associated with multi-transverse-mode operation of VCSELs. Specifically, the capability for achieving multimode synchronization demonstrated here opens the opportunity for multichannel chaotic communications using multi-transverse-mode VCSELs.

The excitation of higher-order modes in VCSELs is often accompanied by polarization switching,[26,27] which affects the laser dynamics. In particular antiphase polarization switching dynamics has been observed in VCSELs.[28] The polarization dynamics of VCSELs with external optical feedback has been studied by several authors.[29–38] Polarization instability is often considered a drawback for the synchronization of VCSELs, but on the other hand it might lead to new ways of transmitting secure information.[39] A new encryption scheme, based on self-pulsating VCSELs that exhibit chaos in both intensity and polarization, was recently proposed theoretically by Scirè *et al.*[40] In that scheme the information is encoded in the phase variables rather than in the intensity of the carrier light beam. The present analysis focuses on the effect of multi-transverse-mode operation on VCSEL synchronization, and no account is taken of polarization effects. The consideration of the role of polarization instabilities in the synchronization of chaotic VCSELs is being undertaken in parallel work.

For unidirectionally coupled edge-emitting laser diodes it has been shown that two schemes of synchronization are possible.[41–45] In the first scheme the lasers are subject to the same amount of total external injection (including optical injection and optical feedback), and the slave laser intensity synchronizes to the master laser intensity with a lag time that is equal to the difference between the external cavity round-trip time τ and the flight time from the master laser to slave laser τ_c. This scheme has been referred to as complete synchronization. In the second scheme the slave laser is subjected to strong optical injection from the master laser, and its intensity synchronizes to the master laser intensity with a lag time equal to flight time τ_c. This scheme has been referred to as injection-locking or lag synchronization. Here we demonstrate numerically that these two types of synchronization also occur in multi-transverse-mode VCSELs.

The model we used in this study is described in Section 2. The model corresponds to a master laser that is subjected to optical feedback from an external mirror, and a slave laser that is a stand-alone laser, subjected only to optical injection from the master laser (open-loop configuration). Section 3 presents the results of the numerical simulations. It is shown that the lasers synchronize either in the complete synchronization regime (when the injection strength is equal to the feedback strength) or in the injection-locking regime (when the injection strength is much larger than the feedback strength). Both regimes can be clearly distinguished by the different lag time between the master laser and the slaver laser dynamics. It is also shown that both synchronization regimes occur independently of the multi-transverse-mode behavior of the master laser. Two different situations are considered: for low injection current the master operates in two transverse modes and the optical feedback induces chaotic in-phase pulses; for larger injection the master laser operates in three transverse modes and the optical feedback induces antiphase oscillations of fundamental and first-order transverse modes. In both cases, for appropriate levels of optical injection, the slave laser synchronizes with the master laser dynamics. Section 4 contains a summary of the results and the conclusions.

2. MODEL

We consider two identical index-guided VCSELs that operate on the same set of transverse modes. The active region of each VCSEL is modeled as a single effective quantum well (QW) of radius a and thickness d_{QW}. Barrier regions of thickness d_b limit the QW region. The injected current is $j(r) = j_0$ for $r < a$ and $j(r) = 0$ otherwise. For the VCSEL circular transverse geometry the appropriate transverse modes are the linearly polarized LP_{mn} modes.[46] To simplify the calculations we consider only three modes having azimuthal symmetry: $\psi_1(r) \equiv \mathrm{LP}_{01}$, $\psi_2(r) \equiv \mathrm{LP}_{02}$, and $\psi_3(r) \equiv \mathrm{LP}_{03}$. The mode profiles are normalized such that $\int_0^\infty |\psi_i|^2 r\,\mathrm{d}r = 1$.

The equations for the slowly varying complex amplitudes $e_i^{m,s}(t)$, the density of carriers confined in the QW region $n_w^{m,s}(r, t)$, and the density of (unconfined) carriers in the barrier region $n_b^{m,s}(r, t)$ are[47–50]

$$\frac{\mathrm{d}e_i^m}{\mathrm{d}t} = \frac{1 + j\alpha}{2}\left(g_i^m - \frac{1}{\tau_{pi}}\right)e_i^m(t) + k_i^m e_i^m(t - \tau) \times \exp(-j\omega_i\tau), \tag{1}$$

$$\frac{\mathrm{d}e_i^s}{\mathrm{d}t} = \frac{1 + j\alpha}{2}\left(g_i^s - \frac{1}{\tau_{pi}}\right)e_i^s(t) + k_i^s e_i^m(t - \tau_c) \times \exp[-j(\omega_i + \Omega)\tau_c], \tag{2}$$

$$\frac{\partial n_b^{m,s}}{\partial t} = \frac{j^{m,s}(r)}{ed_b} - \frac{n_b^{m,s}}{\tau_{cap}} + \frac{V_{\mathrm{QW}}}{V_b}\frac{n_w^{m,s}}{\tau_{esc}} - \frac{n_b^{m,s}}{\tau_n} + D\frac{1}{r}\frac{\partial}{\partial r}\left(r\frac{\partial n_b^{m,s}}{\partial r}\right), \tag{3}$$

$$\frac{\partial n_w^{m,s}}{\partial t} = \frac{V_b}{V_{\mathrm{QW}}}\frac{n_b^{m,s}}{\tau_{cap}} - \frac{n_w^{m,s}}{\tau_{esc}} - \frac{n_w^{m,s}}{\tau_n} - g_0(n_w^{m,s} - n_t) \times \sum |e_i^{m,s}|^2 |\psi_i|^2 + D\frac{1}{r}\frac{\partial}{\partial r}\left(r\frac{\partial n_w^{m,s}}{\partial r}\right). \tag{4}$$

Here the labels m and s correspond to the master and the slave laser, respectively.

The first term on the right-hand side (rhs) of Eqs. (1) and (2) accounts for optical gain, losses, and phase-amplitude coupling. Here, α is the linewidth enhancement factor; τ_{pi} is the photon lifetime for the ith mode; and $g_i^{m,s}$ is the modal gain, $g_i^{m,s} = \int_0^\infty g_0\Gamma_i(n_w^{m,s} - n_t)|\psi_i|^2 r\,\mathrm{d}r$, where g_0 is the gain coefficient; Γ_i is the confinement factor for the ith mode; and n_t is the transparency carrier density.

The second term on the rhs of Eq. (1) takes into account the external optical feedback in the master laser. k_i^m is

the feedback coefficient, τ is the delay time in the external cavity, and ω_i is the optical frequency of the ith mode. The second term on the rhs of Eq. (2) takes into account the optical injection in the slave laser. k_i^s is the injection coefficient of the ith mode, τ_c is the flight time from the master to the slave laser, and Ω is a detuning (since the lasers are identical, only a global shift of the modal frequencies is considered).

The terms on the rhs of Eq. (3) correspond to the rate at which carriers are injected into the barrier region, the rate at which carriers are captured into the QWs, the rate at which carriers escape from the QWs, the carrier loss, and carrier diffusion. The terms on the rhs of Eq. (4) correspond to carriers captured into the QWs, carriers that escape from the QWs, nonradiative carrier loss, carrier loss owing to stimulated recombination, and carrier diffusion. τ_{cap} is the capture time, τ_{esc} is the escape time, τ_n is the carrier lifetime, D is the diffusion coefficient, $V_b = d_b \pi a^2$ ($V_{\mathrm{QW}} = d_{\mathrm{QW}} \pi a^2$) is the volume of the barrier (QW) region.

The effects of carrier capture and escape on the dynamics of VCSELs, which are neglected by many authors (who consider only carriers in the active region), were discussed in detail in Ref. 51. It was shown that carrier capture and escape lead only to a modification of the bias current effectively injected into the active region. Therefore, here we consider τ_{cap} and τ_{esc} as fixed parameters and vary the injection currents of the master and slave lasers, $I_{m,s} = j_0^{m,s} \pi a^2$.

3. NUMERICAL RESULTS

We integrated the equations with typical VCSEL parameters. For simplicity we consider that the lasers have identical internal parameters but can have different injection currents and a nonzero detuning between the optical frequencies of the transverse modes. The laser parameters are[50] $a = 6\ \mu$m, $d_{wq} = 0.024\ \mu$m (three 0.08-μm-thick QWs), $d_b = 1.2\ \mu$m, a refractive-index step of 0.1, $\alpha = 3$, $\tau_{pi} = 2.2$ ps, $g_0 = 4.25 \times 10^{-9}\ \mu\mathrm{m}^3/\mathrm{ns}$, $n_t = 1.33 \times 10^6\ \mu\mathrm{m}^{-3}$, $\Gamma_i = 0.038$, $\tau_{\mathrm{cap}} = 5$ ps, $\tau_{\mathrm{esc}} = 25.5$ ps, $\tau_n = 1.52$ ns, $\omega_2 - \omega_1 = 22.41$ GHz, $\omega_3 - \omega_1 = 59.77$ GHz, and $D = 0.5\ \mu\mathrm{m}^2/\mathrm{ns}$. The time integration step is $\Delta t = 10^{-4}$ ps and the space integration step is $\Delta r = 0.02\ \mu$m. Unless otherwise stated all the transverse modes have the same optical injection strength ($k_i^m = K_m$ and $k_i^s = K_s$). The optical feedback parameters of the master laser are $K_m = 1.6\ \mathrm{ns}^{-1}$, $\tau = 3$ ns, and the flight time is $\tau_c = 2$ ns.

We consider two different values for the master VCSEL injection current I_m. For low injection current the optical feedback induces large chaotic pulses of the dominant fundamental mode LP_{01}, and smaller pulses of the first-order transverse mode LP_{02}. The master laser dynamics is displayed in Fig. 1(a). It can be observed that the modal intensities are in-phase and that the total intensity exhibits large pulses. For larger injection current the master laser operates on three transverse modes [Fig. 2(a)]: the optical feedback induces larger antiphase chaotic oscillations of the LP_{01} and LP_{02} transverse modes, and smaller oscillations of the LP_{03} mode. It can be observed that in this case the total intensity exhibits small oscillations around a constant mean value.

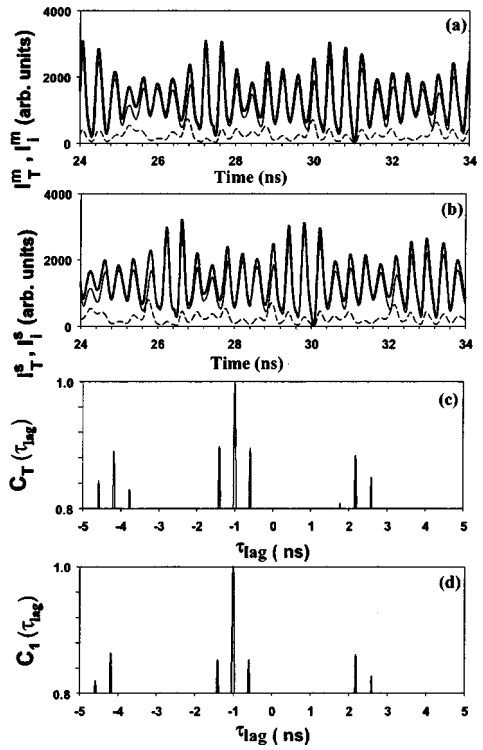

Fig. 1. Complete synchronization when the lasers operate in the in-phase regime. $I_s = I_m = 1.95$ mA and $K_s = K_m = 1.6\ \mathrm{ns}^{-1}$. (a) Master laser total intensity ($I_T^m = \Sigma I_i^m$: thick solid curve) and modal intensities ($I_i^m = |E_i^m|^2$; LP_{01}, thin solid curve; LP_{02}, dashed curve). (b) Slave laser total and modal intensities. (c) Correlation of the total intensities. (d) Correlation of the LP_{01} modal intensities.

Let us first consider a slave laser that has the same injection current as the master laser ($I_s = I_m$), and the same level of optical injection as the master laser ($K_s = K_m$). Figures 1(b) and 2(b) display the slave laser dynamics when the master laser operates in the regime of in-phase and antiphase oscillations, respectively. It can be observed that the feedback-induced oscillations in the master VCSEL are transferred to the slave VCSEL by unidirectional optical injection. Each master laser transverse mode is synchronized with its counterpart in the slave laser, but there is a lag time between them.

To quantify the degree of synchronization and the lag time we computed the correlation function of total intensities C_T and LP_{01} modal intensities C_1:

$$C_{T,1}(\tau_{\mathrm{lag}}) = \frac{\langle [I_{T,1}^m(t + \tau_{\mathrm{lag}}) - \langle I_{T,1}^m \rangle][I_{T,1}^s(t) - \langle I_{T,1}^s \rangle] \rangle}{[\langle (I_{T,1}^m(t) - \langle I_{T,1}^m \rangle)^2 \rangle \langle (I_{T,1}^s(t) - \langle I_{T,1}^s \rangle)^2 \rangle]^{1/2}}. \tag{5}$$

The results are displayed in Figs. 1(c), 1(d), 2(c), and 2(d). Perfect synchronization of both the total and the modal intensities occurs for a lag time of -1 ns, which is equal to $\tau_c - \tau$. This corresponds to the regime of complete synchronization, and, since the value of $\tau_c - \tau$ is negative, the slave laser anticipates the chaotic behavior of the master laser.

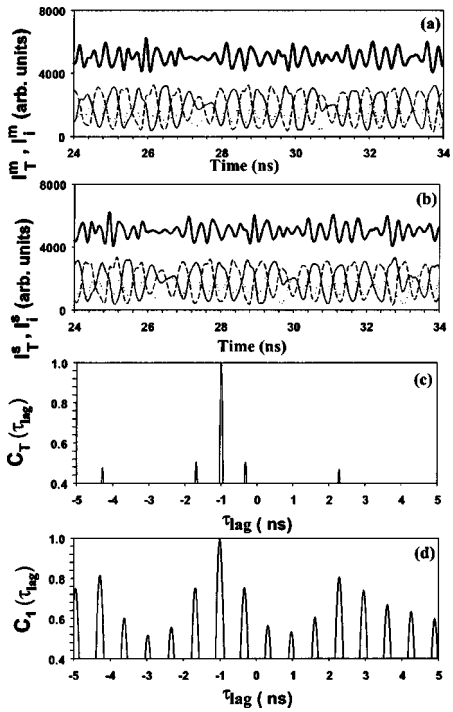

Fig. 2. Complete synchronization when the lasers operate in the antiphase regime. $I_s = I_m = 3.2\,\mathrm{mA}$ and $K_s = K_m = 1.6\,\mathrm{ns}^{-1}$. (a) Master laser total intensity (thick solid curve) and modal intensities (LP_{01}, thin solid curve; LP_{02}, dashed curve; LP_{03}, dot–dash curve). (b) Slave laser total and modal intensities. (c) Correlation of the total intensities. (d) Correlation of the LP_{01} modal intensities.

Next let us consider a strong optical injection level to the slave laser ($K_s \gg K_m$). Figures 3 and 4 display results when the master laser operates in the regime of in-phase and antiphase oscillations, respectively. It can be observed that synchronization of the total and modal intensities also occurs, but now with a lag time of +2 ns between the two lasers, which is equal to τ_c. This corresponds to the regime of injection-locking (or lag) synchronization, where the slave laser lags behind the chaotic behavior of the master laser.

It is interesting to discuss the different dynamic regimes that occur in the slave laser modal intensities as the injection strength K_s increases. These regimes are displayed in Fig. 5. If the injection strength is too small, the slave laser modal intensities are only slightly perturbed [Fig. 5(a)]. If the injection strength is equal to the feedback strength of the master laser, there is complete synchronization [Fig. 5(b)]. An increase of the injection strength leads to a regime in which the slave VCSEL modal intensities exhibit large in-phase pulses [Fig. 5(c)]. Further increase of the injection strength leads to a distortion of the pulses, which gradually become out-of-phase smooth oscillations [Fig. 5(d)]. For even stronger injection the slave VCSEL is synchronized again with the master laser [Fig. 5(e)].

The transition from complete synchronization to injection-locking synchronization for increasing injection strength K_s is illustrated in Fig. 6, which displays the correlation coefficients $C_{T,1}(\tau_c - \tau)$ [Fig. 6(a)] and $C_{T,1}(\tau_c)$ [Fig. 6(b)] as K_s increases. It can be observed that

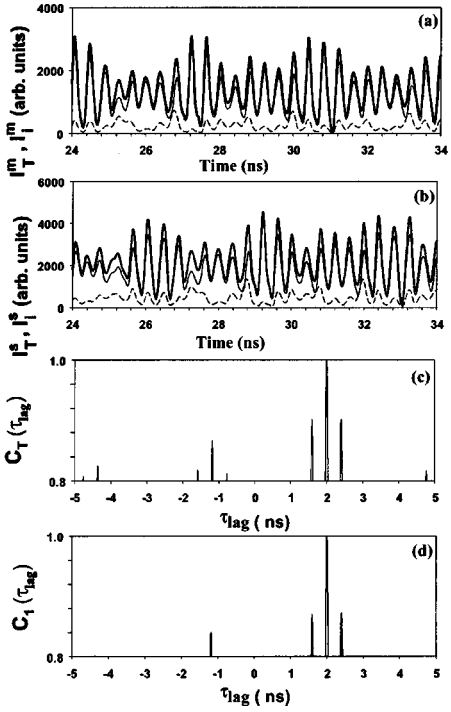

Fig. 3. Injection-locking synchronization when the lasers operate in the in-phase regime. $I_s = I_m = 1.95\,\mathrm{mA}$ and $K_s = 100K_m = 160\,\mathrm{ns}^{-1}$. (a) Master laser total intensity (thick solid curve) and modal intensities (LP_{01}, thin solid curve; LP_{02}, dashed curve). (b) Slave laser total and modal intensities. (c) Correlation of the total intensities. (d) Correlation of the LP_{01} modal intensities.

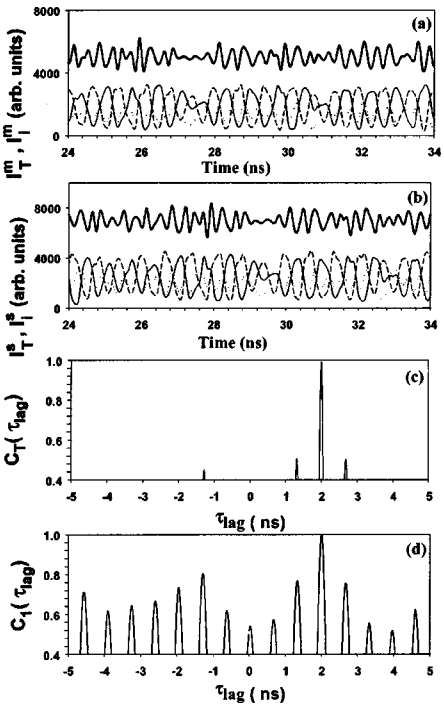

Fig. 4. Injection-locking synchronization when the lasers operate in the antiphase regime. $I_s = I_m = 3.2\,\mathrm{mA}$ and $K_s = 100K_m = 160\,\mathrm{ns}^{-1}$. (a) Master laser total intensity (thick solid curve) and modal intensities (LP_{01}, thin solid curve; LP_{02}, dashed curve; LP_{03}, dot–dash curve). (b) Slave laser total and modal intensities. (c) Correlation of the total intensities. (d) Correlation of the LP_{01} modal intensities.

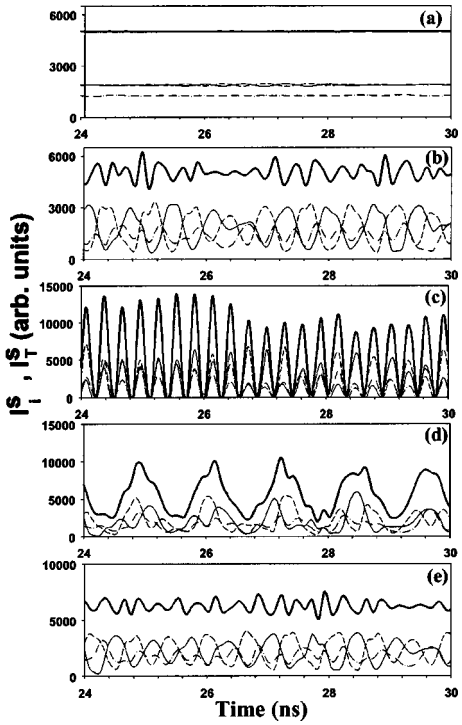

Fig. 5. Dynamics of the slave laser for increasing injection strength. $K_m = 1\ \mathrm{ns}^{-1}$ and $\tau = 1$ ns. K_s = (a) 0.1 ns^{-1}, (b) 1 ns^{-1}, (c) 25 ns^{-1}, (d) 50 ns^{-1}, (e) 100 ns^{-1}. Total intensity, thick solid curve; LP_{01}, thin solid curve; LP_{02}, dashed curve; LP_{03}, dot–dash curve.

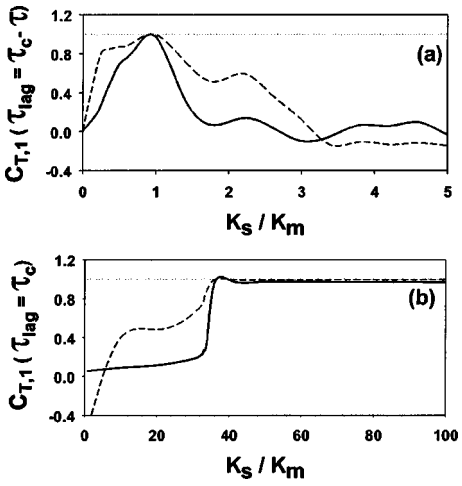

Fig. 6. Correlation coefficient of the total intensities (solid curve) and of the LP_{01} modal intensities (dashed curve) for increasing injection strength. $K_m = 1.6\ \mathrm{ns}^{-1}$. C_T and C_1 are calculated with a lag time of (a) $\tau_c - \tau$ and (b) τ_c.

$C_{T,1}(\tau_c - \tau)$ steadily decrease as K_s increases, indicating that complete synchronization is gradually lost. It can also be observed that $C_{T,1}(\tau_c)$ increase abruptly for $K_s/K_m \sim 40$, indicating a sharp transition to injection-locking synchronization.

Let us now discuss the synchronization regimes when the lasers have different parameters. The simulations indicate that complete synchronization is strongly sensitive to all parameter differences, whereas injection locking is robust under particular differences. First let us consider the case in which the lasers have different injection currents. Figures 7(a) and 7(b) show that, when $I_m > I_s$, good synchronization occurs for large enough optical injection, whereas when $I_m < I_s$ the degree of synchronization is poorer. This is expected because, when the master laser has larger injection current, its output power is larger and therefore there is larger optical injection to the slave laser.

The numerical simulations also show a different sensitivity of injection locking and complete synchronization to a detuning Ω between the two lasers. Figure 8 shows that in the injection-locking regime the effect of detuning is asymmetric: the synchronization is robust to relatively large negative detunings but is lost for similar values of positive detuning. This occurs independently of the transverse-mode behavior: Figs. 8(a) and 8(b) show results when the transverse-mode behavior is in phase (for low injection current), whereas Figs. 8(c) and 8(d) show results when the transverse-mode behavior is antiphase (for larger injection current). Figure 8 also shows that the detuning range in which synchronization can be achieved increases with the optical injection strength. Figure 9 shows that the regime of complete synchronization is sensitive to detuning: the synchronization degrades badly for positive and negative detunings of a few gigahertz. We note that in both regimes the effect of detuning is similar to that previously found in single-mode semiconductor lasers.[43]

The asymmetry of injection-locking behavior with respect to detuning is probably due to the α factor (as in the CW case). The sharp transition to injection-locking synchronization observed in Figs. 6(b), 7(a), 8(b), and 8(d) suggest the existence of hysteretic behavior. We point out that we have not checked for hysteresis as these figures were done with the same initial conditions for all values of K_s or Ω. To check for hysteresis, scans for increasing and decreasing K_s or Ω should be done, using as initial conditions for the next parameter value the final

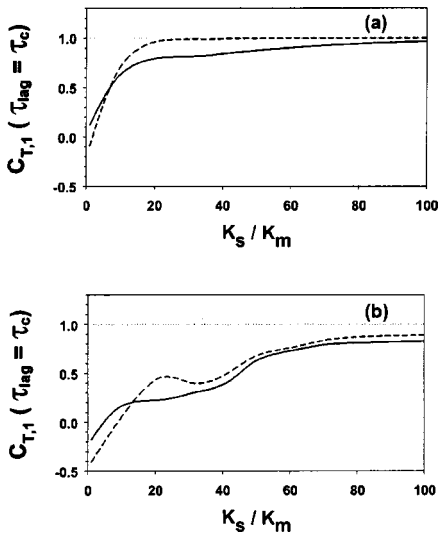

Fig. 7. Correlation coefficient of the total intensities (solid curve) and of the LP_{01} modal intensities (dashed curve) for increasing injection strength. The lasers have different injection currents. (a) $I_m = 3.2$ mA and $I_s = 1.95$ mA. (b) $I_m = 1.95$ mA and $I_s = 3.2$ mA.

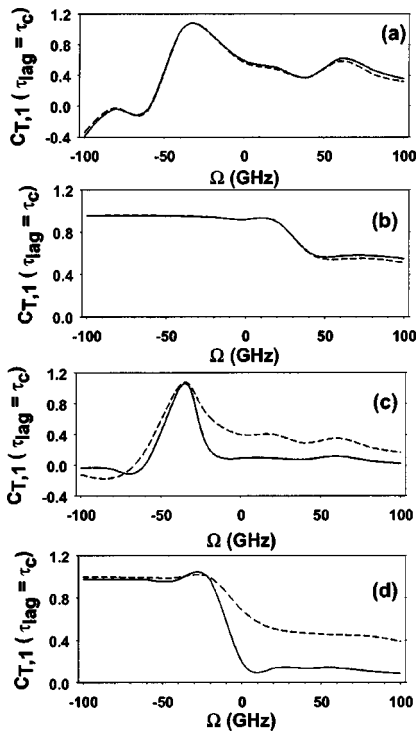

Fig. 8. Correlation of the total intensities (solid curve) and of the LP_{01} modal intensities (dashed curve) as a function of detuning Ω. $K_m = 1.6\,\mathrm{ns}^{-1}$. (a) $I_m = I_s = 1.95$ mA, $K_s = 16\,\mathrm{ns}^{-1}$. (b) $I_m = I_s = 1.95$ mA, $K_s = 50\,\mathrm{ns}^{-1}$. (c) $I_m = I_s = 3.2$ mA, $K_s = 16\,\mathrm{ns}^{-1}$. (d) $I_m = I_s = 3.2$ mA, $K_s = 50\,\mathrm{ns}^{-1}$.

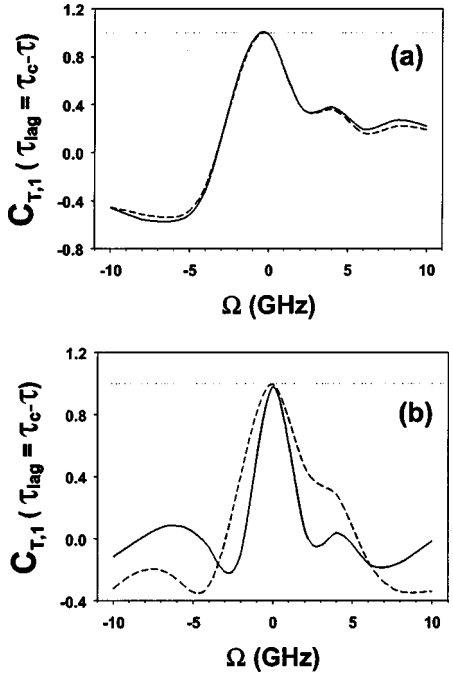

Fig. 9. Correlation of the total intensities (solid curve) and of the LP_{01} modal intensities (dashed curve) as a function of detuning Ω. $K_s = K_m = 1.6\,\mathrm{ns}^{-1}$. (a) $I_m = I_s = 1.95$ mA. (b) $I_m = I_s = 3.2$ mA.

condition of the previous value. This study is left for future work, however, it can be anticipated that multistability and hysteresis would be observed as these are well-known features of diode lasers with CW optical injection.[52–54]

Finally, let us address the case in which the transverse modes of the slave laser receive a different amount of optical injection. As an example, we consider the case in which only the fundamental mode of the slave VCSEL receives optical injection ($k_1^s = K_s$; $k_{2,3}^s = 0$). Figures 10 and 11 display the results for low and large injection currents corresponding to the master laser operating in the in-phase and antiphase regimes respectively.

In Fig. 10 one can observe that weak optical injection [Fig. 10(b)] and strong optical injection [Fig. 10(d)] also induce chaotic oscillations in the slave VCSEL LP_{01} mode (because only the LP_{01} mode receives injection, there is not enough gain for the LP_{02} mode to turn on). The plot of the correlation coefficient C_1 versus the lag time for weak optical injection [Fig. 10(c)] shows that there is no clear lag time between the master laser and the slave laser oscillations. On the other hand, for strong optical injection the plot of C_1 versus τ_{lag} shows a global maximum for $\tau_{lag} = 2$ ns [Fig. 10(e)], indicating injection-locking synchronization.

Similar results are observed for a larger injection current, such that the master laser operates on the antiphase regime [Fig. 11(a)]. Under weak optical injection the slave laser transverse modes also exhibit antiphase oscillations [Fig. 11(b)], but the plot of the correlation coefficients $C_{1,2,3}$ versus τ_{lag} [Fig. 11(c)] reveals no clear lag

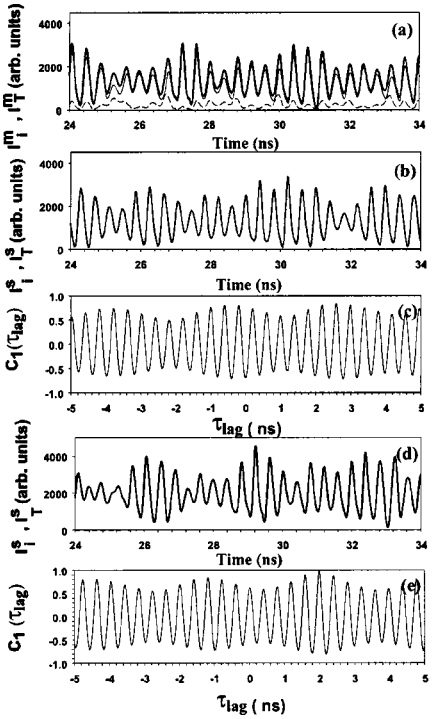

Fig. 10. (a) Total and modal intensities of the master laser. $I_m = 1.95$ mA and $K_m = 1.6\,\mathrm{ns}^{-1}$. (b) Total and modal intensities of the slave laser when $I_s = I_m$, $k_1^s = K_m$, $k_{2,3}^s = 0$. (c) Correlation coefficients. (d) Total and modal intensities of the slave laser when $k_1^s = 100K_m$, $k_{2,3}^s = 0$. (e) Correlation coefficients.

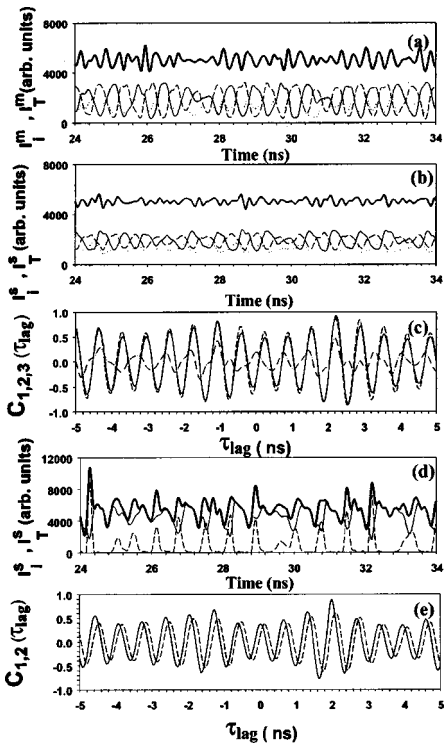

Fig. 11. (a) Total and modal intensities of the master laser. $I_m = 3.2$ mA and $K_m = 1.6\,\mathrm{ns}^{-1}$. (b) Total and modal intensities of the slave laser when $I_s = I_m$, $k_1^s = K_m$, $k_{2,3}^s = 0$. (c) Correlation coefficients. (d) Total and modal intensities of the slave laser when $k_1^s = 100K_m$, $k_{2,3}^s = 0$. (e) Correlation coefficients.

time for which synchronization occurs. Under strong optical injection only the LP_{01} and LP_{02} modes of the slave laser turn on [Fig. 11(d)] and there is again a global maximum of $C_1(\tau_{\mathrm{lag}})$ for $\tau_{\mathrm{lag}} = 2$ ns [Fig. 11(e)], indicating injection-locking synchronization. The LP_{02} transverse mode of the slave laser does not receive optical injection but still synchronizes to its counterpart in the master laser through out-of-phase oscillations with the transverse mode that is subjected to injection. This mechanism for synchronization is similar to that observed experimentally by Fujiwara *et al.*[23] in mutually coupled VCSELs, where only one of the two polarization modes showed synchronized oscillations, and the other polarization component was synchronized as a result of the effect of anticorrelated oscillations.

4. CONCLUSIONS

In conclusion, we have studied numerically the synchronization of unidirectionally coupled VCSELs and have shown that injection-locking and complete synchronization regimes occur in multi-transverse-mode VCSELs. We found that injection-locking synchronization requires high injection powers and thus it is perhaps difficult to observe experimentally, but complete synchronization occurs for weak and moderate optical injection from the master laser and is therefore more amenable to experimental observation. We considered the case in which all the transverse modes of the slave laser receive injection from the master, and the case in which only the fundamental mode receives injection. When all the modes receive injection, each transverse mode of the slave laser synchronizes with its counterpart of the master laser. When only the fundamental transverse mode receives injection, the second-order transverse mode also synchronizes through out-of-phase oscillations.

Although many results reported in this paper for the synchronization of multi-transverse-mode VCSELs are similar to results previously found for conventional multi-longitudinal-mode edge-emitting lasers, there are also important differences that result from the strong correlations between the VCSEL transverse modes. In VCSELs transverse inhomogeneities of the optical field lead to strong transverse hole burning effects, whereas in edge emitters longitudinal hole burning is less relevant because of the fast longitudinal carrier diffusion. As a result, the transverse modes of a VCSEL are strongly coupled to each other, and the longitudinal modes of conventional lasers are weakly coupled to each other. Viktorov and Mandel[12] reported that for multi-longitudinal-mode Fabry–Perot lasers the synchronization of the total output power does not require the synchronization of modal intensities. Because in our VCSEL model the transverse modes are strongly coupled to each other through the carrier dynamics, the synchronization of the total output is observed only when there is synchronization of the modal outputs.

We believe that our results will stimulate further experimental research on VCSEL synchronization, which, because of their multi-transverse-mode behavior, presents new interesting features compared to edge emitters. The opportunity to achieve multiplexed chaotic communications based on multi-transverse-mode synchronization will provide further motivation for experimental exploration of the phenomena examined here. The influence of polarization-switching dynamics offers further opportunities for the exploration and exploitation of VCSEL synchronization and will be treated in future research.

ACKNOWLEDGMENTS

M. S. Torre is supported in part by a grant from Secretaría de Ciencia y Técnica, Universidad Nacional del Centro de la Provincia de Buenos Aires Argentina and Agencia Nacional de Promociòn de Ciencia y Tecnológia grant 3/9598. C. Masoller (cris@fisica.edu.uy) is supported in part by the Engineering and Physical Sciences Research Council, U.K., grant GR/S62239/01 and Comisiòn Sectorial de Investigacion Cientifica and Programa de Desarrollo de las Ciencias Básicas, Uruguay.

REFERENCES

1. G. D. VanWiggeren and R. Roy, "Communication with chaotic lasers," Science **279**, 1198–1200 (1998).
2. J. P. Goedgebuer, L. Larger, and H. Porte, "Optical cryptosystem based on synchronization of hyperchaos generated by a delayed feedback tunable laser diode," Phys. Rev. Lett. **80**, 2249–2252 (1998).
3. C. R. Mirasso, P. Colet, and P. Garcia-Fernandez, "Synchronization of chaotic semiconductor lasers: application to encoded communications," IEEE Photonics Technol. Lett. **8**, 299–301 (1996).
4. V. Ahlers, U. Parlitz, and W. Lauterborn, "Hyperchaotic dy-

namics and synchronization of external-cavity semiconductor lasers," Phys. Rev. E **58**, 7208–7213 (1998).
5. S. Sivaprakasam and K. A. Shore, "Demonstration of optical synchronization of chaotic external-cavity laser diodes," Opt. Lett. **24**, 466–468 (1999).
6. J. K. White and J. V. Moloney, "Multichannel communication using an infinite dimensional spatiotemporal chaotic system," Phys. Rev. A **59**, 2422–2426 (1999).
7. H. Fujino and J. Ohtsubo, "Experimental synchronization of chaotic oscillations in external-cavity semiconductor lasers," Opt. Lett. **25**, 625–627 (2000).
8. I. Fischer, Y. Liu, and P. Davis, "Synchronization of chaotic semiconductor laser dynamics on subnanosecond time scales and its potential for chaos communication," Phys. Rev. A **62**, 011801(R) (2000).
9. Y. Liu, H. F. Chen, J. M. Liu, P. Davis, and T. Aida, "Synchronization of optical-feedback-induced chaos in semiconductor lasers by optical injection," Phys. Rev. A **63**, 031802(R) (2001).
10. A. Uchida, Y. Liu, I. Fischer, P. Davis, and T. Aida, "Chaotic antiphase dynamics and synchronization in multimode semiconductor lasers," Phys. Rev. A **64**, 023801 (2001).
11. C. Masoller, "Anticipation in the synchronization of chaotic semiconductor lasers with optical feedback," Phys. Rev. Lett. **86**, 2782–2785 (2001).
12. E. A. Viktorov and P. Mandel, "Synchronization of two unidirectionally coupled multimode semiconductor lasers," Phys. Rev. A **65**, 015801 (2002).
13. I. V. Koryukin and P. Mandel, "Antiphase dynamics of selectively coupled multimode semiconductor lasers," IEEE J. Quantum Electron. **39**, 1521–1525 (2003).
14. L. Wu and S. Q. Zhu, "Multi-channel communication using chaotic synchronization of multi-mode lasers," Phys. Lett. A **308**, 157–161 (2003).
15. A. Uchida, Y. Liu, and P. Davis, "Characteristics of chaotic masking in synchronized semiconductor lasers," IEEE J. Quantum Electron. **39**, 963–970 (2003).
16. S. Tang and J.-M. Liu, "Effects of message encoding and decoding on synchronized chaotic optical communications," IEEE J. Quantum Electron. **39**, 1468–1475 (2003).
17. J. Paul, S. Sivaprakasam, P. S. Spencer, and K. A. Shore, "Optically modulated chaotic communication scheme with external-cavity length as a key to security," J. Opt. Soc. Am. B **20**, 497–503 (2003).
18. R. Vicente, T. Perez, and C. R. Mirasso, "Open-versus closed-loop performance of synchronized chaotic external-cavity semiconductor lasers," IEEE J. Quantum Electron. **38**, 1197–1204 (2002).
19. M. W. Lee, J. Paul, S. Sivaprakasam, and K. A. Shore, "Comparison of closed-loop and open-loop feedback schemes of message decoding using chaotic laser diodes," Opt. Lett. **28**, 2168–2170 (2003).
20. P. S. Spencer, C. R. Mirasso, P. Colet, and K. A. Shore, "Modeling of optical synchronization of chaotic external-cavity VCSELs," IEEE J. Quantum Electron. **34**, 1673–1679 (1998).
21. P. S. Spencer and C. R. Mirasso, "Analysis of optical chaos synchronization in frequency-detuned external-cavity VCSELs," IEEE J. Quantum Electron. **35**, 803–809 (1999).
22. K. D. Choquette and D. G. Deppe, eds., *Vertical-Cavity Surface-Emitting Lasers*, Proc. SPIE **3003** (1997).
23. N. Fujiwara, Y. Takiguchi, and J. Ohtsubo, "Observation of the synchronization of chaos in mutually injected vertical-cavity surface-emitting semiconductor lasers," Opt. Lett. **28**, 1677–1679 (2003).
24. Y. Hong, M. W. Lee, P. S. Spencer, and K. A. Shore, "Synchronization of chaos in unidirectionally coupled vertical-cavity surface-emitting semiconductor lasers," Opt. Lett. **29**, 1215–1217 (2004).
25. S. F. Yu, P. Shum, and N. Q. Ngo, "Performance of optical chaotic communication systems using multimode vertical cavity surface emitting lasers," Opt. Commun. **200**, 143–152 (2001).
26. C. J. Chang-Hasnain, J. P. Harbison, G. Hasnain, A. C. Von Lehmen, L. T. Florez, and N. G. Stoffel, "Dynamic, polarization, and transverse mode characteristics of vertical cavity surface emitting lasers," IEEE J. Quantum Electron. **27**, 1402–1409 (1991).
27. M. San Miguel, "Polarisation properties of vertical cavity surface emitting lasers," in *Semiconductor Quantum Optoelectronics*, A. Miller, D. M. Finlayson, and M. Ebrahimzadeh, eds. (Institute of Physics, London, 1999), p. 339.
28. S. Bandyopadhyay, Y. Hong, P. S. Spencer, and K. A. Shore, "Experimental observation of anti-phase polarisation dynamics in VCSELS," Opt. Commun. **202**, 145–154 (2002).
29. S. Jiang, Z. Pan, M. Dagenais, R. A. Morgan, and K. Kojima, "High-frequency polarization self-modulation in vertical-cavity surface-emitting lasers," Appl. Phys. Lett. **63**, 3545–3547 (1993).
30. J. Y. Law and G. P. Agrawal, "Effects of optical feedback on static and dynamic characteristics of vertical-cavity surface-emitting lasers," IEEE J. Sel. Top. Quantum Electron. **3**, 353–358 (1997).
31. M. Giudici, S. Balle, T. Ackemann, S. Barland, and J. R. Tredicce, "Polarization dynamics in vertical-cavity surface-emitting lasers with optical feedback: experiment and model," J. Opt. Soc. Am. B **16**, 2114–2123 (1999).
32. C. Masoller and N. B. Abraham, "Low-frequency fluctuations in vertical-cavity surface-emitting semiconductor lasers with optical feedback," Phys. Rev. A **59**, 3021–3031 (1999).
33. M. Sciamanna, C. Masoller, N. B. Abraham, F. Rogister, P. Megret, and M. Blondel, "Different regimes of low-frequency fluctuations in vertical-cavity surface-emitting lasers," J. Opt. Soc. Am. B **20**, 37–44 (2003).
34. M. Sciamanna, C. Masoller, F. Rogister, P. Mégret, N. B. Abraham, and M. Blondel, "Fast pulsing dynamics of a vertical-cavity surface-emitting laser operating in the low-frequency fluctuation regime," Phys. Rev. A **68**, 015805 (2003).
35. M. Sciamanna, K. Panajotov, H. Thienpont, I. Veretennicoff, P. Mégret, and M. Blondel, "Optical feedback induces polarization mode hopping in vertical-cavity surface-emitting lasers," Opt. Lett. **28**, 1543–1545 (2003).
36. M. Sondermann, H. Bohnet, and T. Ackemann, "Low-frequency fluctuations and polarization dynamics in vertical-cavity surface-emitting lasers with isotropic feedback," Phys. Rev. A **67**, 021802 (2003).
37. A. V. Naumenko, N. A. Loiko, M. Sondermann, and T. Ackemann, "Description and analysis of low-frequency fluctuations in vertical-cavity surface-emitting lasers with isotropic optical feedback by a distant reflector," Phys. Rev. A **68**, 033805 (2003).
38. T. Ackemann, M. Sondermann, A. Naumenko, and N. A. Loiko, "Polarization dynamics and low-frequency fluctuations in vertical-cavity surface-emitting lasers subjected to optical feedback," Appl. Phys. B **77**, 739–746 (2003).
39. G. D. VanWiggeren and R. Roy, "Communication with dynamically fluctuating states of light polarization," Phys. Rev. Lett. **88**, 097903 (2002).
40. A. Scirè, J. Mulet, C. R. Mirasso, J. Danckaert, and M. San Miguel, "Polarization message encoding through vectorial chaos synchronization in vertical-cavity surface-emitting lasers," Phys. Rev. Lett. **90**, 113901 (2003).
41. A. Locquet, F. Rogister, M. Sciamanna, P. Mégret, and M. Blondel, "Two types of synchronization in unidirectionally coupled chaotic external-cavity semiconductor lasers," Phys. Rev. E **64**, 045203(R) (2001).
42. A. Locquet, C. Masoller, P. Megret, and M. Blondel, "Comparison of two types of synchronization of external-cavity semiconductor lasers," Opt. Lett. **27**, 31–33 (2002).
43. A. Locquet, C. Masoller, and C. R. Mirasso, "Synchronization regimes of optical-feedback-induced chaos in unidirectionally coupled semiconductor lasers," Phys. Rev. E **65**, 056205 (2002).
44. I. V. Koryukin and P. Mandel, "Two regimes of synchronization in unidirectionally coupled semiconductor lasers," Phys. Rev. E **65**, 026201 (2002).
45. Y. Liu, P. Davis, Y. Takiguchi, T. Aida, S. Saito, and J.-M. Liu, "Injection locking and synchronization of periodic and chaotic signals in semiconductor lasers," IEEE J. Quantum Electron. **39**, 269–278 (2003).

46. M. S. Sodha and A. K. Ghatak, *Inhomogeneous Optical Waveguides* (Plenum, New York, 1977).
47. A. Valle, J. Sarma, and K. A. Shore, "Dynamics of transverse mode competition in vertical cavity surface emitting laser diodes," Opt. Commun. **115**, 297–302 (1995).
48. A. Valle, J. Sarma, and K. A. Shore, "Spatial holeburning effects on the dynamics of vertical cavity surface-emitting laser-diodes," IEEE J. Quantum Electron. **31**, 1423–1431 (1995).
49. R. Lang and K. Kobayashi, "External optical feedback effects on semiconductor injection laser properties," IEEE J. Quantum Electron. **QE-16**, 347–355 (1980).
50. M. S. Torre, C. Masoller, and P. Mandel, "Transverse-mode dynamics in vertical-cavity surface-emitting lasers with optical feedback," Phys. Rev. A **66**, 053817 (2002).
51. M. S. Torre and C. Masoller, "Effects of carrier transport on the transverse-mode selection of index-guided vertical-cavity surface-emitting lasers," Opt. Commun. **202**, 311–318 (2002).
52. A. Gavrielides, V. Kovanis, P. M. Varangis, T. Erneux, and G. Lythe, "Coexisting periodic attractors in injection-locked diode lasers," Quantum Semiclassic. Opt. **9**, 785–796 (1997).
53. S. Wieczorek, B. Krauskopf, and D. Lenstra, "Mechanisms for multistability in a semiconductor laser with optical injection," Opt. Commun. **183**, 215–226 (2000).
54. M. Nizette, "Temporal dynamics of driven nonlinear optical systems," Ph.D. Dissertation (Université Libre de Bruxelles, Brussels, Belgium, 2003).